

Research Article

Open Access



The effect of accessibility to acid sites in Y zeolites on ring opening reaction in light cycle oil hydrocracking

Ping Yang¹, Siyang Yan², Ning He², Hong Nie¹, Luyao Guo², Guang Xiong², Naixin Wang¹, Jiayu Liu^{2*}, Mingfeng Li^{1*}

¹Department of National Energy R&D Center of Petroleum Refining Technology, SINOPEC Research Institute of Petroleum Processing Co., Ltd., Beijing 100083, China.

²Department of State Key Laboratory of Fine Chemicals, Frontier Science Center for Smart Materials, School of Chemical Engineering, Dalian University of Technology, Dalian 116024, Liaoning, China.

***Correspondence to:** Dr. Jiayu Liu, Department of State Key Laboratory of Fine Chemicals, Frontier Science Center for Smart Materials, School of Chemical Engineering, Dalian University of Technology, No. 2 Linggong Road, Ganjingzi District, Dalian 116024, Liaoning, China. E-mail: liujiayu@dlut.edu.cn; Dr. Mingfeng Li, Department of National Energy R&D Center of Petroleum Refining Technology, SINOPEC Research Institute of Petroleum Processing Co., Ltd., No. 18 Xueyuan Road, Haidian District, Beijing 100083, China. E-mail: limf.ripp@sinopec.com

How to cite this article: Yang, P.; Yan, S.; He, N.; Nie, H.; Guo, L.; Xiong, G.; Wang, N.; Liu, J.; Li, M. The effect of accessibility to acid sites in Y zeolites on ring opening reaction in light cycle oil hydrocracking. *Chem. Synth.* **2025**, *5*, 24. <https://dx.doi.org/10.20517/cs.2024.133>

Received: 19 Sep 2024 **First Decision:** 29 Sep 2024 **Revised:** 5 Oct 2024 **Accepted:** 18 Oct 2024 **Published:** 13 Feb 2025

Academic Editor: Jun Xu **Copy Editor:** Pei-Yun Wang **Production Editor:** Pei-Yun Wang

Abstract

The light cycle oil (LCO) hydrocracking process converts polycyclic aromatics into highly valuable light aromatics such as benzene, toluene, xylene (BTX), in accordance with the requirements of low-carbon development and high-quality transformation from oil refining to chemical industry. The accessibility of acid sites is a critical factor that impacts LCO conversion and BTX yield. Initially, the fine structure and molecular size of the typical polycyclic aromatics in LCO and their hydrogenation reaction intermediates were investigated through gas chromatography-mass spectrometry (GC-MS) analysis and density functional theory (DFT) calculations. Three porous Y zeolites with comparable Si/Al molar atomic ratios and pyridine (Py)-measured Brønsted acid amounts were chosen as an acidic component to prepare NiMo/(Al₂O₃ + HY) catalysts. The acid accessibility of HY zeolite was characterized via dual-beam infrared spectroscopy using 2,4,6-tri-tert-butylpyridine (2,4,6-TTBP) and trihexylamine (THA) as probe molecules, and the LCO hydrocracking performance was evaluated on a fixed-bed reactor. The results revealed that bicyclic aromatic hydrocarbons featuring multiple, short side chains such as dimethylnaphthalene and trimethylnaphthalene are the main components of LCO, with sizes larger than those of HY zeolite micropores.



© The Author(s) 2025. **Open Access** This article is licensed under a Creative Commons Attribution 4.0 International License (<https://creativecommons.org/licenses/by/4.0/>), which permits unrestricted use, sharing, adaptation, distribution and reproduction in any medium or format, for any purpose, even commercially, as long as you give appropriate credit to the original author(s) and the source, provide a link to the Creative Commons license, and indicate if changes were made.



There is a strong positive correlation between LCO conversion and ring-opening rate of polycyclic aromatics and cycloalkanes in LCO. Among these three HY zeolite catalysts, the ring-opening rates of polycyclic aromatics and cycloalkanes, and the yields of C₆-C₁₂ aromatics and BTX increased in the order of HY1 < HY2 < HY3, which is consistent with external surface acidity measured by THA as the probe molecule.

Keywords: LCO hydrocracking, zeolite, acidity, accessibility, adsorption in FTIR

INTRODUCTION

Light cycle oil (LCO) is a main byproduct derived from the fluid catalytic cracking (FCC) process, known for its characteristic features including high density, elevated levels of sulfur and nitrogen impurities coupled with a low cetane number. With up to 90% total aromatic content comprising mainly bicyclic and tricyclic polycyclic^[1-4], LCO has been utilized as a blending component for diesel production through processes such as hydro-refining or hydro-upgrading technologies. However, growing environmental and health regulations concerning polycyclic aromatic hydrocarbon (PAH) content in clean fuels have become more stringent. Currently, the Euro VI Emission Standard limits it to no more than 8% (m/m), while the China VI Vehicle Emission Standard sets an even lower maximum at 7% (m/m). Anticipated further tightening of these restrictions has sparked increased interest in the utilization of LCO through hydrocracking processes to produce highly valuable chemicals such as benzene, toluene, xylene (BTX)^[2,3,5-14].

Under the hydrocracking conditions [Figure 1], LCO initially undergoes hydrogenation saturation reactions of PAHs and the removal of sulfur and nitrogen impurities to obtain hydrotreated LCO (HDT-LCO), which is enriched in tetralin-based monocyclic aromatics hydrocarbons. It then enters the hydrocracking reaction zone where the tetralin-based monocyclic aromatic hydrocarbons experience ring-opening and cracking tandem reaction, yielding BTX. The ring-opening involving tetralin-based monocyclic aromatics hydrocarbons is a crucial and essential process step that enhances LCO conversion and BTX selectivity during this process.

In the presence of traditional transition metal sulfide-zeolite bifunctional hydrocracking catalysts, the ring-opening reaction of tetralin-based monocyclic aromatics is typically catalyzed by Brønsted acid sites (BAS) located on zeolite^[15,16]. Owing to its suitable pore structure and adjustable acidity, HY zeolite is commonly utilized as a catalyst acidic component for LCO hydrocracking in both industry and academic research. The quantity, strength, density, and accessibility of BAS on HY zeolite are primary factors affecting the activity and selectivity of ring-opening reaction^[17]. Due to the small dimensions of HY zeolite micropores (0.74 nm × 0.74 nm), the diffusion of PAHs and tetralin-based monocyclic aromatics in LCO and HDT-LCO into zeolite micropores still presents challenges^[2,18]. Therefore, improving acid accessibility is particularly crucial, and methods such as increasing pore size^[19], introducing mesopores^[8,20] and reducing crystal size^[21] have been recognized as effective approaches. Meanwhile, precise characterization of acid accessibility in zeolites is also essential. Currently, it is commonly characterized using Fourier transform infrared spectroscopy (FTIR) with various alkaline probe molecules such as pyridine (Py), 2,6-dimethylpyridine, and 2,6-di-tert-butylpyridine^[22-24]. However, the identification of aromatics in LCO and HDT-LCO focuses on the hydrocarbon types but lacks systematic studies on specific molecular structures and dimensions. This could lead to conventional probe molecules providing inaccurate acidity information that may impact or even mislead catalyst design efforts. Therefore, it is essential to identify suitable alkaline probe molecules that can accurately measure zeolite acidity while having a reliable correlation with catalytic performance^[25].



Figure 1. The simplified reaction process of LCO hydrocracking to produce BTX. LCO: Light cycle oil; BTX: benzene, toluene, xylene.

In this study, the chemical composition and structure of typical PAHs in LCO and their partially hydrogen-saturated products in HDT-LCO were initially determined at the molecular level and then the hydrocracking process was studied through a fixed-bed high-throughput reactor. Simultaneously, three hierarchical porous HY zeolites with similar Si/Al molar atomic ratios and total Brønsted amounts (measured by Py as probe molecule) were chosen as acidic components of catalysts. The acidities of HY zeolites were characterized through a dual-beam FTIR (DB-FTIR) with three alkaline probe molecules: Py, 2,4,6-tri-tert-butylpyridine (2,4,6-TTBP) and trihexylamine (THA), each possessing different molecular sizes and configuration. Based on DB-FTIR and density functional theory (DFT) calculation results, the accessibility of acid sites in the three HY zeolites was compared, and the effects of acid accessibilities on ring-opening performance of PAHs and BTX yields during LCO hydrocracking were also investigated. The assessment of acid accessibility, adapted to the size and adsorption states of reactant molecules, is essential for precise design and development of high-performance zeolite catalytic materials and hydrocracking catalysts.

EXPERIMENTAL

LCO and HDT-LCO characterization

To obtain the molecular size of aromatic hydrocarbons in LCO and HDT-LCO, hydrocarbon composition and carbon number distribution were analyzed in detail. The hydrocarbon composition is measured by standard methods ASTM D 2425 and ASTM D 8276 with Agilent 7890A/MSD5977 gas chromatography-mass spectrometry (GC-MS). The carbon number distribution of hydrocarbons is measured by JEOL JMS-T200GC-TOF gas chromatography-field ionization source time of flight mass spectrometry (GC-FI TOFMS). A 0.2 μ L sample was injected onto a HP-5 MS column (30 m \times 0.25 mm inner diameter \times 0.25 μ m film thickness), which was held at 60 $^{\circ}$ C for 2 min, ramped to 300 $^{\circ}$ C at 20 $^{\circ}$ C/min, and then held at a final temperature for 5 min. The GC-TOF MS interface temperature was at 300 $^{\circ}$ C. The field ionization emitter was at 10 kV voltage, with a 10 mA emitter current on a 10 μ m emitter.

Catalyst preparation

Three hierarchical porous HY zeolites with similar Si/Al molar atomic ratios but different pore distributions, denoted as HY1, HY2, and HY3, were selected as acidic components of catalysts [Supplementary Table 1]. Their atomic molar ratios of Si to Al range from 3 to 5.

Subsequently, a composite carrier of zeolite and alumina with a dry mass ratio of 60 wt% HY zeolite and 40 wt% binder was prepared as follows: the HY zeolite mixed with pseudo-boehmite (Sasol Co., Germany) and homogenized, and then extruded using a single-screw extruder (the BONNOT Co., America) through a die with a diameter of 1.6 mm. The resulting extrudates were dried at 393 K for 3 h followed by calcination at 873 K under an air atmosphere for an additional 3 h.

Finally, the NiMo/(HY- Al_2O_3) catalysts were prepared by impregnating molybdenum trioxide, nickel carbonate hydroxide, and phosphoric acid aqueous solution onto the supports with 15 wt% MoO_3 , 3 wt% NiO and 3 wt% P_2O_5 . Subsequently, they were dried at 393 K for 3 h and calcined at 723 K under an air atmosphere for another 3 h to obtain corresponding catalysts labeled as C1, C2, and C3 [Supplementary Table 2].

Zeolites and catalysts characterization

The crystal structures of zeolite were characterized through X-ray diffraction (XRD) using a German Siemens D5005 X-ray diffractometer, with Cu K_{α} radiation source and a scanning range of 2θ from 4° to 36° , at a tube voltage of 40 kV and tube current of 40 mA.

The specific surface areas and pore size distributions were determined by N_2 adsorption-desorption isotherms at 77 K, performed on an ASAP 2400 automatic adsorption analyzer produced by Micromeritics. Zeolite samples (20-40 mesh) were first vacuum-treated at 350°C for 4 h. N_2 was used as the adsorbate, and adsorption was performed at -196°C until reaching a state of static adsorption equilibrium. The specific surface area of the molecular sieve was calculated using the Brunauer-Emmett-Teller (BET) equation, and the pore size distribution was determined using the Barrett-Joyner-Halenda (BJH) model.

The aluminum distribution of the zeolites was obtained by using ^{27}Al magic angle spinning nuclear magnetic resonance (MAS NMR) on a Bruker Avance 500 NMR spectrometer.

A DB-FTIR using the Nicolet IS 50 FTIR spectrometer was employed to qualitatively characterize the acidic sites of the zeolites by the adsorption of alkaline probe molecules Py, 2,4,6-TTBPY and THA. The zeolite powder was pressed into a self-supporting thin wafer (1.5 cm^2), which was placed in the sample beam of the DB-FTIR; the reference beam was not placed with the sample. Then, the sample was decontaminated at 400°C under vacuum (10^{-2} Pa) for 4 h. After the pretreatment, the sample was cooled down to room temperature for adsorption. The spectra of the adsorbed probe molecules were obtained as follows: firstly, excess vapor-phase probe molecules were introduced at room temperature, and then desorbed at 150°C for 30 min. The spectra were obtained by subtracting the reference spectrum from the measured sample spectra. The amount of acid is calculated by the integral area of the corresponding band of the spectrum^[26].

Performance evaluation

The catalyst performance evaluation was conducted on a 16-channel fixed-bed high-throughput evaluation equipment with HDT-LCO containing 1,000 ppm S and 500 ppm N as feedstock. Typically, a 2 mL catalyst (16-20 mesh) was loaded in a tubular reactor, and inert SiO_2 (40-60 mesh) was filled on both sides of the reactor constant temperature zone. The catalyst needs to be pre-sulfurized before the reaction, using kerosene containing 2.5% dimethyl disulfide (DMDS) as the sulfurization oil at 573 K and 6.4 MPa for 8 h. After sulfurization, switch to the reaction oil and adjust the reaction pressure to 5.5 MPa, and raise the temperature to reaction temperature in the range of 663 to 683 K. After stabilizing for 48 h, the gas products were quantitatively analyzed using online gas chromatography, and the liquid products were analyzed off-line.

The LCO conversion and ring-opening rate were determined by

The conversion of LCO:

$$\text{Conversion} = \frac{m_{in} - m_{out}}{m_{in}} \times 100\% \quad (1)$$

The ring-opening rate of PAHs and polycyclic cycloalkanes in LCO:

$$\text{Ring opening rate} = \frac{C_{in} - C_{out}}{C_{in}} \times 100\% \quad (2)$$

Table 1. Hydrocarbon compositions of LCO and HDT-LCO

Mass fraction of hydrocarbons/%	LCO	HDT-LCO
Paraffins	7.8	9.9
Mono-cycloalkanes	0.9	0.9
Bicyclic cycloalkanes	1.8	4.7
Tricyclic cycloalkanes	0.5	1.6
Total cycloalkanes	3.2	7.2
Total aromatic hydrocarbons	89.0	82.9
Alkylbenzenes	9.7	10.4
Tetralins or indans	6.8	31.7
Indenes and/or C _n H _{2n-10}	1.5	8.4
Total monocyclic aromatic hydrocarbons	18.0	50.5
Naphthalenes	38.4	10.8
Acenaphthenes and/or C _n H _{2n-14}	11.8	10.8
Fluorenes and/or C _n H _{2n-16}	10.7	7.8
Total bicyclic aromatic hydrocarbons	60.9	29.4
Tricyclic aromatic hydrocarbons	10.1	3.0

LCO: Light cycle oil; HDT-LCO: hydrotreated LCO.

where m_{in} and m_{out} refer to the mass fractions of the components in the feedstock and products with boiling point higher than 478 K, respectively. C_{in} and C_{out} refer to the total amounts of cycloalkanes and aromatic hydrocarbons containing two or more rings in the feedstock and products, respectively. It is worth noting that during the hydrocracking process, tricyclic aromatic hydrocarbons in LCO will undergo hydrosaturation, ring-opening and cracking reactions to transform into bicyclic aromatic hydrocarbons. Similarly, tricyclic cycloalkanes will also be converted into bicyclic cycloalkanes through ring-opening and cracking reactions. However, accurately distinguishing whether these bicyclic aromatic hydrocarbons and cycloalkanes originate from LCO feedstock or reaction generation remains challenging. Since they are intermediate products, a simplified calculation method is adopted in Equation (2). This method does not account for the ring-opening rate of tricyclic aromatic hydrocarbons and cycloalkanes to bicyclic aromatic hydrocarbons and cycloalkanes, which may lead to an underestimation of the ring-opening rate.

RESULTS AND DISCUSSION

Aromatic distributions and typical molecular structures in LCO and HDT-LCO

The hydrocarbon compositions of LCO and HDT-LCO are presented in Table 1, showing that the total aromatic content in LCO is 89.0%. Among these aromatic hydrocarbons, the bicyclic aromatic hydrocarbons account for 68.4% of the total, with a content of 60.9%. Bicyclic aromatic hydrocarbons mainly include naphthalene, acenaphthene, fluorene, and their alkyl-substituted derivatives according to molecular structure, among which naphthalene and alkyl-substituted naphthalenes are the most abundant. In contrast to LCO, the remaining PAHs including bicyclic and tricyclic aromatic hydrocarbons in HDT-LCO show a significant decrease, while the levels of monocyclic aromatic hydrocarbons, cycloalkanes, and alkanes exhibit a notable increase. Among these changes, the most substantial rise is observed in the content of monocyclic aromatic hydrocarbons, particularly those tetralin or indane-like structures. As previously mentioned, certain PAHs present in LCO undergo partial hydro-saturation reaction during the hydrotreating process and are converted into tetralin-like monocyclic aromatic hydrocarbons, which serve as primary reactants for subsequent hydrocracking reactions.

To obtain the molecular structure, we conducted the carbon number distributions of bicyclic aromatic hydrocarbons in LCO and monocyclic aromatic hydrocarbons in corresponding HDT-LCO. As illustrated in [Figure 2], alkylated naphthalenes in LCO predominantly exhibit a carbon number ranging from 11 to 14, while the alkylated acenaphthenes and fluorenes mainly fall within the range of 14 to 16. This suggests that the bicyclic aromatic hydrocarbons in LCO are predominantly alkyl-substituted with 1-4 side chain carbon atoms. Similarly, monocyclic aromatic hydrocarbons in HDT-LCO mainly consist of tetralin-like compounds with a carbon number ranging from 11 to 14. This is attributed to the fact that polycyclic aromatic compounds primarily undergo hydro-saturation reactions during the hydrotreating process, while the dealkation and cracking of alkyl side chains are almost negligible.

GC-MS is utilized to further identify the predominant bicyclic aromatic hydrocarbons in LCO for calculating their molecule sizes, with a specific focus on alkyl-substituted naphthalenes with carbon atom numbers of 12 and 13. As illustrated in Figure 3, alkyl-substituted naphthalenes with C₁₂ predominantly consist of various isomers including dimethylnaphthalene, along with a minor presence of ethylnaphthalene. Similarly, alkyl-substituted naphthalenes with C₁₃ primarily consist of diverse isomers such as trimethylnaphthalene, accompanied by a small quantity of methylethyl naphthalene and propylnaphthalene. These findings indicate that the PAHs in LCO mainly comprise polysubstituted alkyl-aromatic compounds featuring short side chains, which undergo transformation into the corresponding tetralin-like monocyclic aromatic hydrocarbons in HDT-LCO during the hydrotreating process.

Table 2 presents the three-dimensional dimensions of the predominant alkyl-naphthalenes and corresponding alkyltetralins in C₁₂ and C₁₃. It is evident that these molecules are significantly larger than the micropores of HY zeolite (0.74 nm × 0.74 nm), rendering them unable to penetrate the pores of the zeolite.

Quantitative analysis of physicochemical property and BAS accessibility in HY zeolites

XRD characterization of the three HY zeolite samples was conducted and the results were depicted in Figure 4A. All the samples display typical diffraction peaks of the FAU topology structure zeolite. No significant additional peaks are observable.

The aluminum coordination states on the three HY zeolites are illustrated in Figure 4B. The peak with a chemical shift (δ) at approximately 60 ppm corresponds to the tetrahedrally coordinated framework aluminum (FAL), while the peak with δ at around 0 ppm belongs to the octahedrally coordinated Extra-FAL (EFAL). The assignment of the peaks with chemical shifts between 30 and 50 ppm is still under debate, but they are generally considered as distorted tetrahedral or penta-coordinated EFAL. As depicted in Figure 4B, all the HY zeolites predominantly contain FAL, with a minor presence of EFAL. Among them, HY2 exhibits the lowest content of EFAL.

Table 3 and Supplementary Figure 1 show the textural properties of the HY zeolites. The specific surface areas of these zeolites range from 651 to 700 m²/g, and the pore volumes vary from 0.355 to 0.400 cm³/g. The mesoporous specific surface area and mesoporous pore volume increase gradually from HY1 to HY3. It can be seen from Figure 4C that there is a gradual increase in the proportion of mesopores (primarily 10-40 nm) in zeolites from HY1 to HY3, which could influence the accessibility of acidic centers.

FTIR is usually employed to qualitatively characterize the acidic sites of the zeolites. Many basic molecules, such as small alkaline probe molecules (ammonia and Py) and large probe molecules (multi-alkylated Py or other organic amine molecules), can be used to characterize the acidity of samples. The selection of different alkaline probe molecules can provide diverse information on acidity. Therefore, it is desirable and highly

Table 2. The three-dimensional dimensions of typical C₁₂ and C₁₃ naphthalenes and tetralins

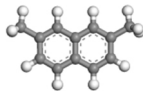
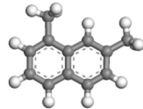
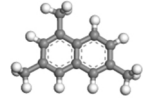
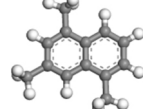
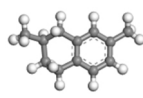
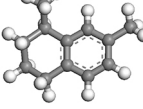
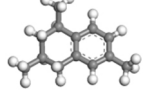
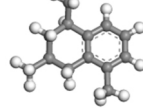
Molecule	Structure	a × b × c / nm × nm × nm
2,7-dimethylnaphthalene		1.10 × 0.72 × 0.40
1,7-dimethylnaphthalene		1.01 × 0.83 × 0.41
1,3,6-trimethylnaphthalene		1.09 × 0.85 × 0.40
1,3,5-trimethylnaphthalene		0.99 × 0.87 × 0.40
2,7-dimethyltetralin		1.14 × 0.72 × 0.53
1,7-dimethyltetralin		1.03 × 0.83 × 0.53
1,3,6-trimethyltetralin		1.12 × 0.85 × 0.52
1,3,5-trimethyltetralin		1.02 × 0.89 × 0.53

Table 3. Texture properties of HY zeolites

Zeolite	Specific surface area/(m ² /g)			Pore volume/(cm ³ /g)		
	S _{BET}	S _{Micro}	S _{meso}	V _{pore}	V _{micro}	V _{meso}
HY1	700	670	31	0.355	0.310	0.045
HY2	641	608	33	0.365	0.287	0.078
HY3	651	619	63	0.460	0.290	0.170

BET: Brunauer-Emmett-Teller.

challenging to choose the appropriate alkaline probe molecule based on the chemical properties and molecular size of reactants.

Three alkaline probe molecules with different molecular sizes and chemical properties were selected to assess the accessibility of acid sites in HY zeolites, aiming to investigate their impacts on the performance of LCO hydrocracking for light aromatic hydrocarbon production. The adsorption energies on the external surface BAS were calculated by DFT (B3LYP/6-31 + G^{**}). Table 4 shows the total acid amount and external

Table 4. Acid properties of HY zeolites

Zeolites	Total acid amount mL NH ₃ /g	Total acid amount on BAS by Py/(μ mol/g)	External surface acid amount of BAS by 2,4,6-TTBPY/(μ mol/g)	External surface acid amount of BAS by THA/(μ mol/g)
HY1	36.77	101	27	40
HY2	36.58	109	5	48
HY3	25.97	92	3	87

BAS: Brønsted acid sites; Py: pyridine; 2,4,6-TTBPY: 2,4,6-tri-tert-butylpyridine; THA: trihexylamine.

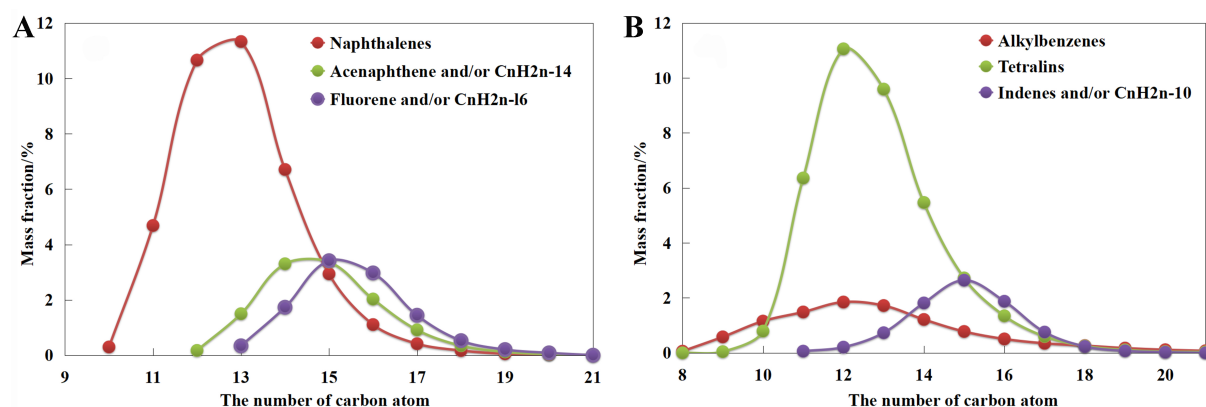


Figure 2. (A) Carbon number distribution of bicyclic aromatic hydrocarbons in LCO and (B) monocyclic aromatic hydrocarbons in HDT-LCO. LCO: Light cycle oil; HDT-LCO: hydrotreated LCO.

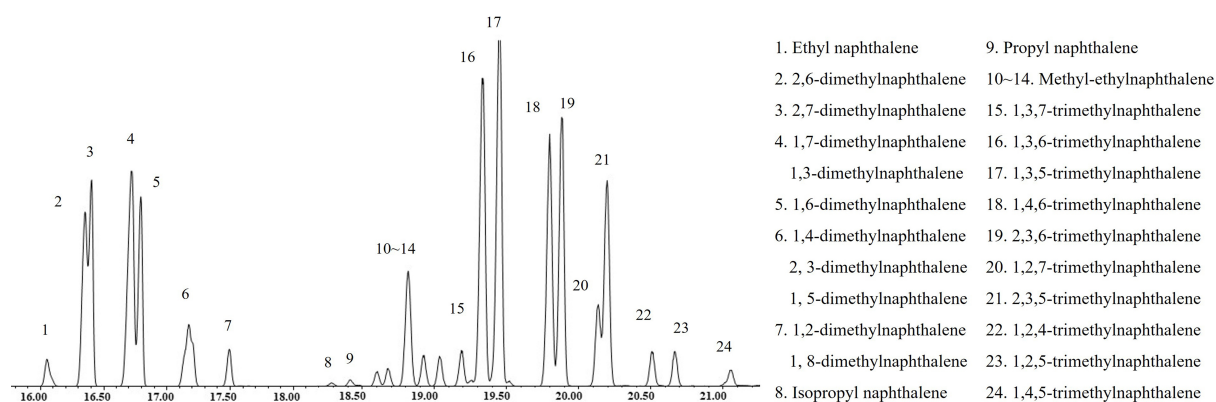


Figure 3. Main molecular structure of naphthalenes in LCO. LCO: Light cycle oil.

surface Brønsted acid amount of the three HY zeolites. Considering its molecular size (~ 0.57 nm), Py can approach almost all the acidic sites of the zeolites. Thus, the acid amount measured by Py is defined as the total acid amount. Additionally, 2,4,6-TTBPY (~ 1.1 nm) and THA (~ 1.4 nm) were chosen as probe molecules, resembling the aromatics in LCO and HDT-LCO [Table 2], which can only approach the acidic sites on the external surface of the zeolites due to their large molecular size. The acid amount measured by these molecules is defined as external surface acidity.

As shown in Figure 5, $1,540\text{ cm}^{-1}$ of Py adsorption, $3,377\text{ cm}^{-1}$ of 2,4,6-TTBPY adsorption, and $1,450\text{ cm}^{-1}$ of THA adsorption on zeolites are attributed to the presence of BAS. Table 4 shows that the total Brønsted acid amount measured by Py gradually decreases from HY1 to HY3, while the external surface Brønsted acid

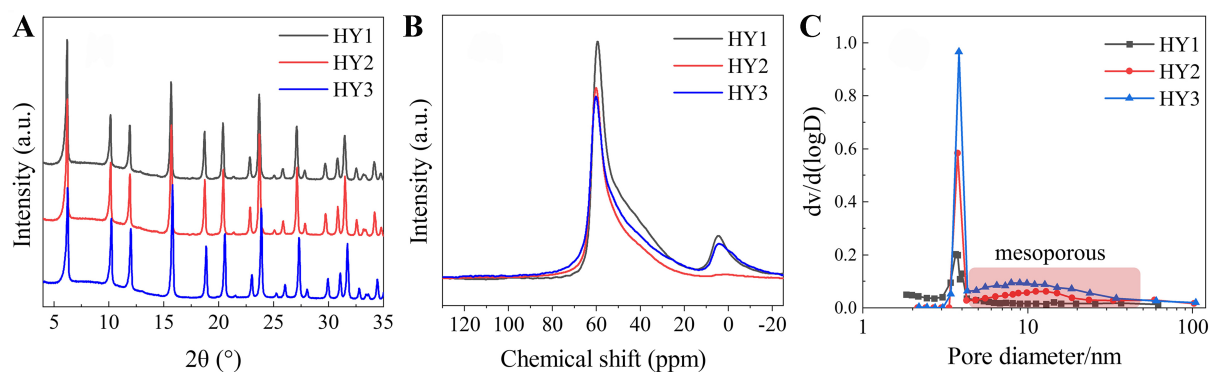


Figure 4. (A) XRD pattern, (B) ^{27}Al MAS NMR spectra, (C) pore size distribution of HY zeolites. XRD: X-ray diffraction; MAS NMR: magic angle spinning nuclear magnetic resonance.

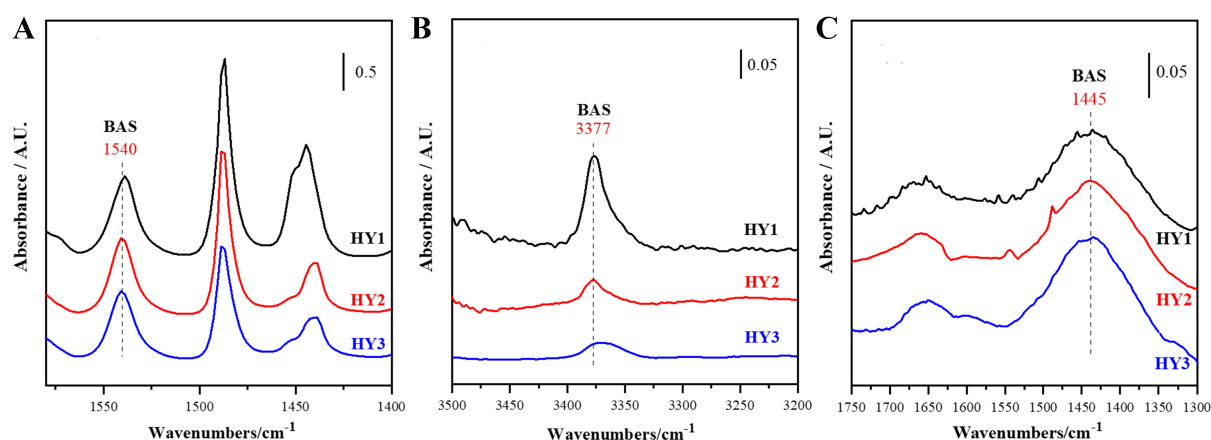


Figure 5. Acid amount on BAS measured by (A) Py and external surface BAS measured by (B) 2,4,6-TTBPpy and (C) THA of the three HY zeolites. BAS: Brønsted acid sites; Py: pyridine; 2,4,6-TTBPpy: 2,4,6-tri-tert-butylpyridine; THA: trihexylamine.

amount measured by THA shows a gradual increase. The external surface Brønsted acid amount measured by 2,4,6-TTBPpy is exceedingly low and also exhibits a gradual decrease. The three alkaline probe molecules provide totally different information on acidity of these HY zeolites.

The calculation results from [Figure 6](#) and [Table 5](#) indicate that Py exhibits strong ion adsorption with BAS. Among the probe molecules, THA possesses the largest molecular size, which hinders its entry into zeolite channels. However, due to its quasi-planar structure, it exhibits relatively small steric hindrance with the zeolite framework, resulting in relatively strong ion adsorption on the surface BAS. In contrast, 2,4,6-TTBPpy has a smaller molecular size with THA, but its increased steric hindrance between the three tert-butyl branches and the zeolite framework prevents nitrogen on the Py ring from interacting with the BAS and leads to the reduced adsorption energy. Therefore, the Brønsted acid amount measured by 2,4,6-TTBPpy would be underestimated.

LCO hydrocracking process and the effects of BAS accessibility on catalytic performance

As stated in [Figure 1](#), monocyclic aromatic hydrocarbons in HDT-LCO undergo isomerization, ring-opening, and cracking reactions on the hydrocracking catalysts to yield desirable BTX products. Additionally, side reactions such as over-cracking, excessive hydrosaturation, and polymerization coking are also facilitated. Based on their distinct boiling points, the products are classified into C_1 - C_4 gases,

Table 5. Adsorption energy and some key bond lengths of Py, 2,4,6-TTBPpy and THA adsorbed on HY zeolites

Probe molecule	$E_{ads}/kcal/mol$	Bond length/ \AA	
		N-H	H-O
Py	-36.14	1.06	1.64
2,4,6-TTBPpy	-8.64	3.06	0.98
THA	-33.89	1.06	1.71

Py: Pyridine; 2,4,6-TTBPpy: 2,4,6-tri-tert-butylpyridine; THA: trihexylamine.

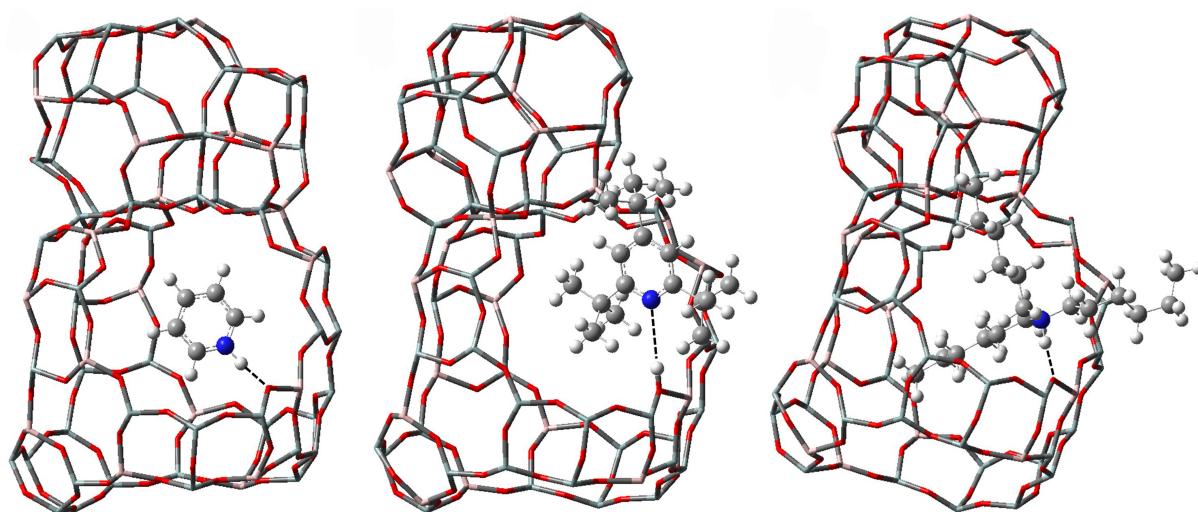


Figure 6. Structures of Py, 2,4,6-TTBPpy and THA adsorbed on BAS of HY zeolite. Py: Pyridine; 2,4,6-TTBPpy: 2,4,6-tri-tert-butylpyridine; THA: trihexylamine; BAS: Brønsted acid sites.

naphtha ranging from C_5 to 478 K, and unconverted diesel above 478 K. The naphtha products are further divided into C_5 - C_{12} paraffins, C_5 - C_{12} cycloalkanes, and C_6 - C_{12} aromatic hydrocarbons according to carbon number and molecular structure.

A comparative analysis was conducted to investigate the hydrocracking process of HDT-LCO, focusing on changes of hydrocarbons in unconverted diesel and distributions of product (Catalyst 1, C1). As illustrated in Figure 7A, there is a significant reduction in levels of monocyclic aromatic hydrocarbons, such as alkylbenzenes, indanes or tetralins, and indenes compared to the HDT-LCO feedstock. Additionally, an increase in reaction temperature leads to reduced paraffin contents along with cycloalkanes, alkylbenzenes and indanes or tetralins. However, the contents of bicyclic and tricyclic aromatic hydrocarbons initially decrease before subsequently rising. This phenomenon may be attributed to thermodynamic equilibrium limitations on hydrosaturation reaction for aromatic hydrocarbons at elevated temperatures.

Under the experimental conditions [Figure 7B], C_6 - C_{12} aromatic hydrocarbons are identified as the main products. With rising reaction temperature, there is a continuous increase in the yield of C_6 - C_{12} aromatic hydrocarbons, a gradual increase in the yield of C_1 - C_4 gaseous products, and a slight decrease in the yield of C_6 - C_{12} cycloalkanes. The yield of C_6 - C_{12} paraffins initially increases before exhibiting a decreasing trend.

These observations indicate that, within the hydrocracking reaction zone, minimal amounts of cycloalkanes and paraffins in HDT-LCO undergo cracking reactions, and ring-opening reactions of tetralin-like monocyclic aromatic hydrocarbons and cracking reaction of corresponding ring-opening products

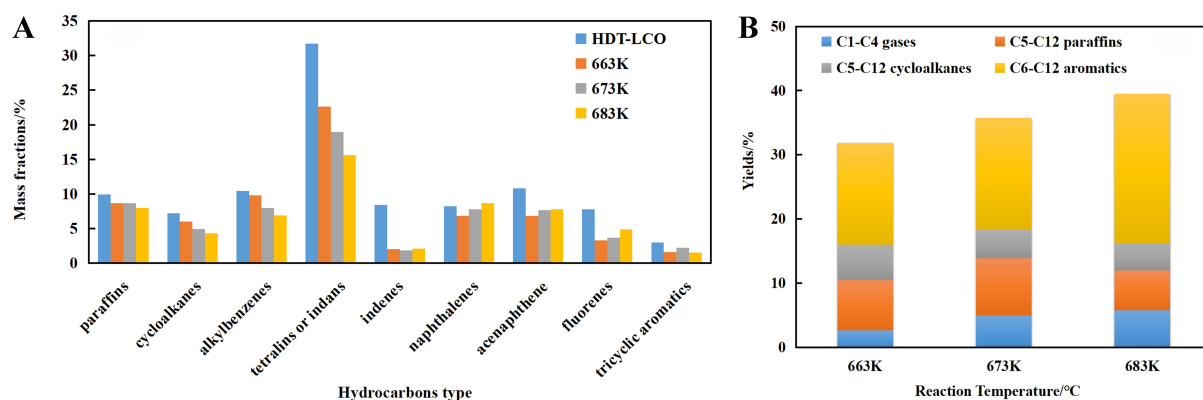


Figure 7. (A) Changes of hydrocarbons in unconverted diesel and (B) distributions of product on C1 catalyst.

predominantly occur, leading to the formation of C_6 - C_{12} aromatic hydrocarbons along with minor amount of gaseous and light saturated hydrocarbons.

A comprehensive comparison of product distribution over the three catalysts is presented in Table 6, demonstrating a gradual increase in the conversion of HDT-LCO from C1 to C3. Moreover, the conversion was enhanced with rising reaction temperature. The hydrocarbon changes in unconverted diesel and product distribution at 683 K on the three catalysts are further illustrated in Figure 8. As shown in Figure 8A, the aromatic hydrocarbons in unconverted diesel on C3 catalyst, including monocyclic, bicyclic, and tricyclic compounds, are the lowest, followed by C2 and C1. Consequently, as depicted in Figure 8B, the yields of C_1 - C_4 gases, C_5 - C_{12} alkanes, C_5 - C_{12} cycloalkanes and C_6 - C_{12} aromatic hydrocarbons produced by the C3 catalyst are the highest among all catalysts examined. Additionally, C2 catalyst exhibits slightly higher C_5 - C_{12} cycloalkanes and C_6 - C_{12} aromatic hydrocarbons than those on C1.

Although the LCO conversions and product yields differ among the three catalysts, there is a notable increase in the LCO conversion as the ring-opening rate of PAHs and polycyclic cycloalkanes in LCO increases [Figure 9]. A strong linear correlation is evident, further affirming that the ring-opening reaction plays a crucial role in determining the reaction activity during LCO hydrocracking processing.

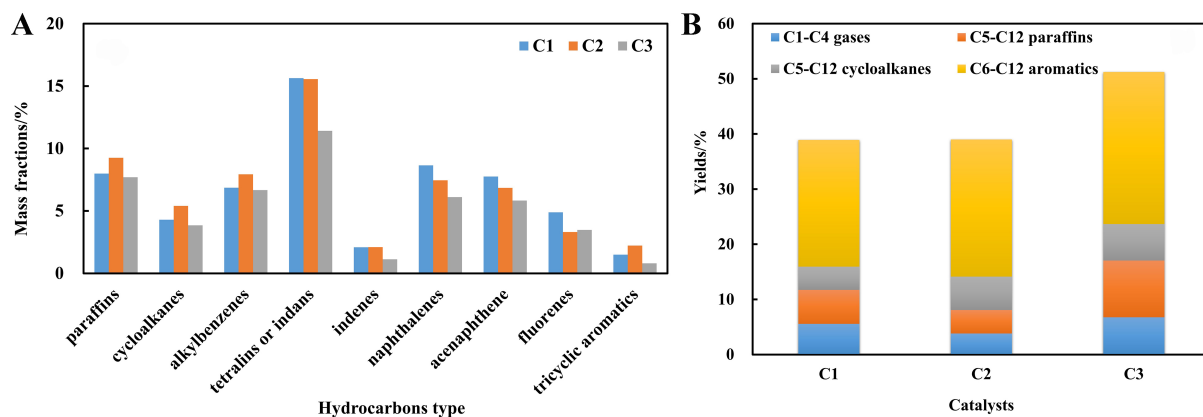
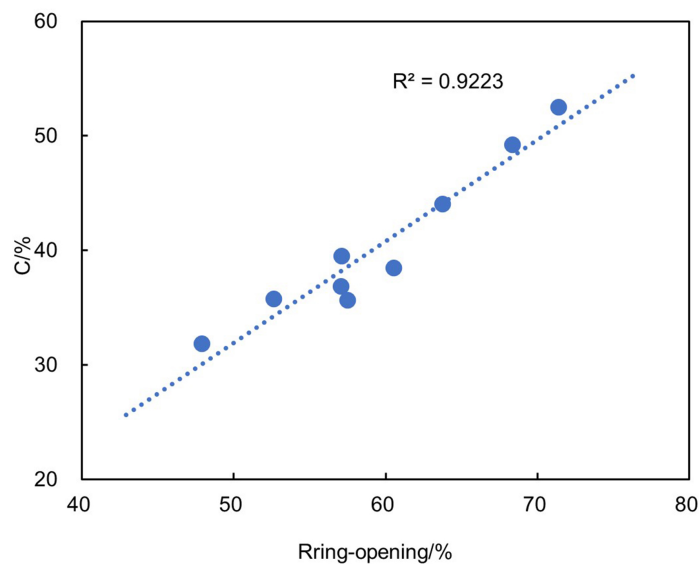
Figure 10 revealed a strong positive correlation between the amount of accessibility Brønsted acid on HY zeolites determined by THA and the ring-opening rate for PAHs and polycyclic cycloalkanes, as well as the yield of C_6 - C_{12} benzenes and BTX. As a heterogeneous catalytic process, the initial and key step of the ring-opening reaction involves diffusion and adsorption of reactant molecules onto acidic sites. While both THA and 2,4,6-TTBPY are unable to enter HY zeolite micropores, it is worth noting that THA molecules exhibit smaller steric hindrance compared to 2,4,6-TTBPY. This makes it more similar to the adsorption behavior of aromatics in LCO and HDT-LCO (the C-H and O-H bond strengths of 2,7-dimethylteralin adsorbed on HY zeolites are 2.08 and 0.99 Å, respectively). Therefore, THA is better suited for characterizing the accessibility of aromatics in LCO and HDT-LCO to the acidic sites over HY zeolite hydrocracking catalysts.

CONCLUSIONS

The hydrocracking of LCO to produce light aromatic hydrocarbons is an effective approach for addressing excess diesel production capacity and facilitating the high-quality transformation of refineries into chemicals. LCO primarily consists of bicyclic aromatics with multiple, short side chains ranging from C_1 to C_4 , such as dimethylnaphthalene and trimethylnaphthalene. These compounds are transformed into

Table 6. Variation of product distribution with temperature on three catalysts

Yields/%	C1			C2			C3		
	663 K	673 K	683 K	663 K	673 K	683 K	663 K	673 K	683 K
C ₁ -C ₄ gases	2.61	4.76	5.56	3.18	3.24	3.82	3.55	5.09	6.76
Naphtha	29.15	30.37	33.37	33.64	34.09	35.18	40.61	43.81	44.46
Unconverted diesel	68.24	64.86	61.07	63.17	62.67	61.01	55.85	51.09	48.77

**Figure 8.** Influences of catalysts on (A) changes of hydrocarbons in unconverted diesel and (B) distributions of product.**Figure 9.** Relationship between the ring-opening rate of PAHs and LCO conversion. PAHs: Polycyclic aromatic hydrocarbons; LCO: light cycle oil.

monocyclic aromatic hydrocarbons such as alkyltetralins with minimal disruption to the side chain after hydrotreating. During the subsequent hydrocracking process, the alkyltetralins undergo ring opening and cracking tandem reaction, yielding C₁-C₄ gases, C₅-C₁₂ paraffins, C₅-C₁₂ cycloalkanes and C₆-C₁₂ light aromatics, with the latter being the main products. There is a strong positive correlation between the conversion and the ring-opening rate of PAHs and polycyclic cycloalkanes in LCO.

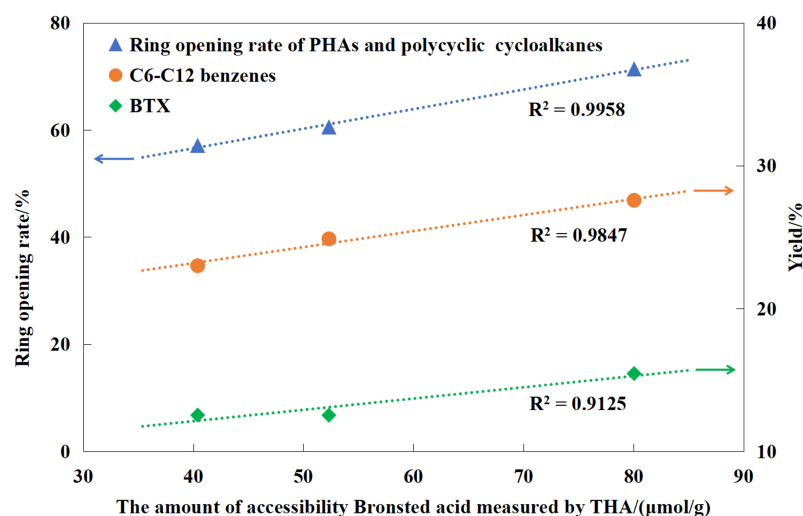


Figure 10. Relationship between ring-opening rate, light aromatic hydrocarbons yield and acid amount of accessibility BAS. BAS: Brønsted acid sites.

The dimensions of typical alkyl naphthalenes in LCO and the corresponding alkyl tetralins in HDT-LCO are larger than those of micropores over HY zeolites. This makes it difficult for them to effectively enter the pores for adsorption onto BAS or subsequent reaction. Therefore, three hierarchical porous HY zeolites possessing comparable Si/Al molar atomic ratios and BAS were selected to investigate acid accessibility and their effects on LCO hydrocracking. The analysis of THA adsorption in FTIR indicates that the proportion and quantity of the external surface BAS on HY zeolites increase in the order of HY1 < HY2 < HY3, which is in good consistency with product distribution, particularly evident through the increasing trend of ring-opening rate of PAHs and polycyclic cycloalkanes, yields of C₆-C₁₂ light aromatic hydrocarbons and BTX. By employing THA in combination with FTIR, a strong correlation has been established between acid accessibility and the performance of LCO hydrocracking on HY zeolite catalysts. These findings can provide fundamental information for the development of high-performance hydrocracking catalysts and technologies.

DECLARATIONS

Authors' contributions

Carried out the preparation, physical property characterization and tests of the catalysts, and prepared the draft manuscript: Yang, P.

Performed FTIR characterization of the catalysts and prepared the draft manuscript: Yan, S.

Performed FTIR characterization of the catalysts: Guo, L.

Performed the DFT calculation: He, N.

Corrected the manuscript: Xiong, G.

Performed GC-MS characterization of LCO and HDT-LCO: Wang, N.

Planned the study: Liu, J.; Li, M.; Nie, H.

Availability of data and materials

The datasets generated and/or analyzed during the current study are not publicly available due to the involvement of trade secrets, but are available from the corresponding author upon reasonable request.

Financial support and sponsorship

This research is supported by the National Key Research and Development Program of China (2022YFA1504402), the National Energy R&D Center of Petroleum Refining Technology (RIPP, SINOPEC) and “the Fundamental Research Funds for the Central Universities” (DUT22LAB601, etc.).

Conflicts of interest

Yang, P.; Nie, H.; Wang, N.; and Li, M. are affiliated with SINOPEC Research Institute of Petroleum Processing Co., Ltd, while the other authors have declared that they have no conflicts of interest.

Ethical approval and consent to participate

Not applicable.

Consent for publication

Not applicable.

Copyright

© The Author(s) 2025.

REFERENCES

1. Ramteke, A. V.; Bhatia, D.; Pant, K. Conversion of light cycle oil to benzene and alkylated monoaromatics over monometallic and bimetallic CoMo catalysts in the presence of hydrogen donor. *Fuel* **2023**, *342*, 127737. DOI
2. Corma, A.; González-Alfaro, V.; Orchillés, A. Decalin and tetralin as probe molecules for cracking and hydrotreating the light cycle oil. *J. Catal.* **2001**, *200*, 34-44. DOI
3. Peng, C.; Huang, X.; Duan, X.; et al. Direct production of high octane gasoline and ULSD blend stocks by LCO hydrocracking. *Catal. Today*. **2016**, *271*, 149-53. DOI
4. Zhang, L.; Tang, X.; Li, J.; Yang, J.; Dai, G. Extraction and separation of polycyclic aromatic hydrocarbons from catalytic cracking diesel. *J. Chem. Eng. Data*. **2023**, *68*, 393-404. DOI
5. Miao, P.; Miao, J.; Guo, Y.; Lin, C.; Zhu, X.; Li, C. Efficient conversion of light cycle oil into gasoline with a combined hydrogenation and catalytic cracking process: effect of pre-distillation. *Energy Fuels*. **2020**, *34*, 12505-16. DOI
6. Xin, L.; Liu, X.; Chen, X.; Feng, X.; Liu, Y.; Yang, C. Efficient conversion of light cycle oil into high-octane-number gasoline and light olefins over a mesoporous ZSM-5 catalyst. *Energy Fuels*. **2017**, *31*, 6968-76. DOI
7. Laredo, G. C.; Pérez-Romo, P.; Escobar, J.; Garcia-Gutierrez, J. L.; Vega-Merino, P. M. Light cycle oil upgrading to benzene, toluene, and xylenes by hydrocracking: studies using model mixtures. *Ind. Eng. Chem. Res.* **2017**, *56*, 10939-48. DOI
8. Oh, Y.; Noh, H.; Park, H.; Han, H.; Nguyen, T.; Lee, J. K. Molecular-size selective hydroconversion of FCC light cycle oil into petrochemical light aromatic hydrocarbons. *Catal. Today*. **2020**, *352*, 329-36. DOI
9. Cao, Z.; Zhang, X.; Xu, C.; et al. Selective hydrocracking of light cycle oil into high-octane gasoline over bi-functional catalysts. *J. Energy. Chem.* **2021**, *52*, 41-50. DOI
10. Oh, Y.; Shin, J.; Noh, H.; et al. Selective hydrotreating and hydrocracking of FCC light cycle oil into high-value light aromatic hydrocarbons. *Appl. Catal. A. Gen.* **2019**, *577*, 86-98. DOI
11. Escalona, G.; Rai, A.; Betancourt, P.; Sinha, A. K. Selective poly-aromatics saturation and ring opening during hydroprocessing of light cycle oil over sulfided Ni-Mo/SiO₂-Al₂O₃ catalyst. *Fuel* **2018**, *219*, 270-8. DOI
12. Chen, F.; Zhang, G.; Weng, X.; et al. High value utilization of inferior diesel for BTX production: mechanisms, catalysts, conditions and challenges. *Appl. Catal. A. Gen.* **2021**, *616*, 118095. DOI
13. Qi, L.; Peng, C.; Cheng, Z.; Zhou, Z. Structure-performance relationship of NiMo/Al₂O₃-HY catalysts in selective hydrocracking of poly-aromatics to mono-aromatics. *Chem. Eng. Sci.* **2022**, *263*, 118121. DOI
14. Peng, C.; Zhou, Z.; Cheng, Z.; Fang, X. Upgrading of light cycle oil to high-octane gasoline through selective hydrocracking over non-noble metal bifunctional catalysts. *Energy Fuels*. **2019**, *33*, 1090-7. DOI
15. Du, H.; Fairbridge, C.; Yang, H.; Ring, Z. The chemistry of selective ring-opening catalysts. *Appl. Catal. A. Gen.* **2005**, *294*, 1-21. DOI
16. Santikunaporn, M.; Herrera, J.; Jongpatiwut, S.; Resasco, D.; Alvarez, W.; Sughrue, E. Ring opening of decalin and tetralin on HY and Pt/HY zeolite catalysts. *J. Catal.* **2004**, *228*, 100-13. DOI
17. Lee, J.; Choi, Y.; Shin, J.; Lee, J. K. Selective hydrocracking of tetralin for light aromatic hydrocarbons. *Catal. Today*. **2016**, *265*, 144-53. DOI
18. Arribas, M. A.; Martínez, A.; Sastre, G. Simultaneous hydrogenation and ring opening of aromatics for diesel upgrading on Pt/zeolite catalysts. The influence of zeolite pore topology and reactant on catalyst performance. *Stud. Surf. Sci. Catal.* **2002**, *142*, 1015-22. DOI

19. Arribas, M.; Corma, A.; Díaz-cabañas, M.; Martínez, A. Hydrogenation and ring opening of Tetralin over bifunctional catalysts based on the new ITQ-21 zeolite. *Appl. Catal. A. Gen.* **2004**, *273*, 277-86. DOI
20. Qi, J.; Guo, Y.; Jia, H.; et al. Unpredictable properties of industrial HY zeolite for tetralin hydrocracking. *Fuel. Proc. Technol.* **2023**, *240*, 107586. DOI
21. Sharma, P.; Iguchi, Y.; Sekine, Y.; Kikuchi, E.; Matsukata, M. 42 Hydroisomerization of tetralin on zeolite beta: influence of crystal size. *Stud. Surf. Sci. Catal.* **2003**, *145*, 219-22. DOI
22. Nesterenko, N.; Thibault-Starzyk, F.; Montouillout, V.; et al. Accessibility of the acid sites in dealuminated small-pore mordenites studied by FTIR of co-adsorbed alkylpyridines and CO. *Micropor. Mesopor. Mat.* **2004**, *71*, 157-66. DOI
23. Mlekodaj, K.; Tarach, K.; Datka, J.; Góra-Marek, K.; Makowski, W. Porosity and accessibility of acid sites in desilicated ZSM-5 zeolites studied using adsorption of probe molecules. *Micropor. Mesopor. Mat.* **2014**, *183*, 54-61. DOI
24. Thibault-Starzyk, F.; Stan, I.; Abelló, S.; et al. Quantification of enhanced acid site accessibility in hierarchical zeolites - The accessibility index. *J. Catal.* **2009**, *264*, 11-4. DOI
25. Zhang, L.; Hu, Q.; Qin, Y.; et al. Optimizing the accessibility of zeolite Y on FCC catalyst to improve heavy oil conversion capacity. *Micropor. Mesopor. Mat.* **2023**, *359*, 112627. DOI
26. Lakiss, L.; Vicente, A.; Gilson, J. P.; et al. Probing the Brønsted acidity of the external surface of faujasite-type zeolites. *Chemphyschem* **2020**, *21*, 1873-81. DOI PubMed



Ping Yang

Ping Yang obtained her master's degree in Chemical Technology from the Sinopec Research Institute of Petroleum Processing Co., Ltd. (RIPP) in 2011. In 2021, she was awarded the title of Associate Research Fellow. Her expertise includes research on the hydrocracking reaction and the development of catalytic materials and catalysts in hydrocracking processing of oil refining.



Jiaxu Liu

Jiaxu Liu obtained his bachelor's and Ph.D. degrees in Chemical Engineering from Dalian University of Technology in 2007 and 2013, respectively. He then worked as a postdoc fellow in ETH, Zurich (2015). In December 2023, he was promoted to full professor of the School for Chemical Engineering, Dalian University of Technology. His expertise includes heterogeneous catalysis in clean synthesis of fine chemicals, design of hierarchically structured zeolites for catalysis, and developing operando dual beam FT-IR spectroscopy to accurately characterize heterogeneous catalysis processes under reaction conditions.



Mingfeng Li

Prof. Mingfeng Li obtained his Ph.D. in Chemical technology in 2001. He is a professorate senior engineer, doctoral supervisor, and member of the Chinese Society of Chemical Industry. He serves as the president of the Sinopec Research Institute of Petroleum Processing Co., Ltd. (RIPP) and is the director of the “Special Committee on Hydrocarbon Resource Evaluation, Processing and Utilization” of the Chinese Society of Chemical Industry, and director of the “Special Committee on Carbon Neutrality” of the Chinese Society of Petroleum. His current research interests focus on Gasoline and Diesel Quality Improvement, Chemical Recycling of Waste Plastics, Hydrogen Energy Production and Utilization, and Dual-Carbon Accounting in the Petrochemical Industry.